

## AIRPLANE SCALING METHODS

Ștefan ANTON<sup>1</sup>, Petrișor PÂRVU<sup>2</sup>

<sup>1</sup> University “Politehnica” of Bucharest, Faculty of Aerospace Engineering, PhD candidate, E-mail: stefan.anton05@gmail.com

<sup>2</sup> University “Politehnica” of Bucharest, Aerospace Sciences Department, Associate Professor, E-mail: petrisor.parvu@upb.ro

Corresponding author: Ștefan ANTON, E-mail: stefan.anton05@gmail.com

**Abstract.** In this paper a scaling method for similar Unmanned Aerial Vehicles (UAV) is presented. The ultimate purpose is to generate reduced model plane geometric and mass parameters that can be modified so that the full-scale UAV would have the same dynamic behavior as the model plane. This is achieved by using the relative density factor similitude criteria. Doing so, the result from test flights of the model plane can be extrapolated to the dynamic behavior of the full-scale UAV. This paper is using the dynamic model from Etkin [1], with additions from Nelson [2] and Pârnu [3], in order to obtain a dynamic behavior assessment for a model plane (low Reynolds number). The model plane dynamic assessment includes the step response for 1-degree elevator deflection applied to the reference movement – horizontal rectilinear unaccelerated flight, fixed control surfaces.

**Key words:** UAV dynamic model, scaled plane, similitude criteria, scale factor, low Reynolds number.

### 1. INTRODUCTION

Different aircraft behave differently during flight. A large transport aircraft flies in a different manner than a fighter jet. A business jet flies in a different manner than a small unmanned aerial vehicle. Even two different transport aircraft fly differently. Things like the mass of the aircraft, the geometry of the wings, the distribution of mass in the aircraft, the type of propulsion, the shape of the control surfaces and many other factors affect how a certain aircraft behaves during flight. It is important to be able to understand how a certain aircraft fly. This topic is studied in the field of flight dynamics.

In recent years, development in use and versatility of UAVs, generated need of rapidly developing for improved performances, especially greater payload, and range. This can be achieved by scaling existing successfully flown configurations, but the downsize is the possibility to deteriorate the flying qualities. To preserve the good flying qualities of the flown configuration, similitude criteria must be applied. This will assure also less effort in designing the autopilot.

Plane scaling involves geometric scaling in all aspects including the gaps between the command surfaces. Similitude criteria are summarized in reference [4]. Currently there are many authors that use Froude similitude in order to scale a plane. But also, Reynolds number must be observed for similar aerodynamic forces and moments. The similarity of the Reynolds number must be fulfilled in order to have the same transition point on the airfoil, the thickness of the boundary layer and possible interference by the interaction of the Reynolds number with Mach number (compressibility effects). As distribution of mass properties on a given configuration is subjected to many restrictions, the two mentioned criteria cannot be met, usually, only by scaling.

One important aspect in defining airplanes dynamics is the correct determination of the stability and command derivatives [5]. For UAVs this determination can be done with low cost sensors, using extended Kalman filters, as explained in [6], or using Genetic Algorithm Optimized Method, as in [7].

In this paper we will consider only the most usual movements of airplanes, horizontal level flight, climb and descend and takeoff and landing. More complex movements, as the ones described in [8], are not considered. The research done in this paper follows the general guidelines of aircraft design depicted in [9].

Due to the complexity of the autopilot design, as described in [10], rapid prototyping of a whole series of similar UAVs can benefit of the results of this research if we can obtain same stability and control matrices, which are inputs in the process of design and optimization of the control system, as shown in [11].

In this paper the relative density factor is used, because the model plane obtained has the same damping factor  $\zeta_{sp}$  as the reference plane. This is demonstrated only for short period mode. In order to evaluate the dynamic behavior, step response was considered. Model plane considered parameters are:  $f_s$  (scale factor),  $p_1$  (mass ratio) and  $p_2$  (inertia moment ratio). The mathematical model was obtained from [1] with additions from [2], [12] and [3]. The longitudinal movement equations are shown in equations (1). The lateral-directional equations used are shown in (2).

$$\begin{bmatrix} \Delta \dot{u} \\ \dot{w} \\ \dot{q} \\ \Delta \dot{\theta} \end{bmatrix} = \begin{bmatrix} \frac{X_u}{m} & \frac{X_w}{m} & 0 & -g \cdot \cos \theta \\ \frac{Z_u}{m-Z_{\dot{w}}} & \frac{Z_w}{m-Z_{\dot{w}}} & \frac{Z_q+m \cdot u_0}{m-Z_{\dot{w}}} & \frac{-mg \cdot \sin \theta}{m-Z_{\dot{w}}} \\ \frac{1}{I_y} \left[ M_u + \frac{M_{\dot{w}} Z_u}{m-Z_{\dot{w}}} \right] & \frac{1}{I_y} \left[ M_w + \frac{M_{\dot{w}} Z_w}{m-Z_{\dot{w}}} \right] & \frac{1}{I_y} \left[ M_q + \frac{M_{\dot{w}} (Z_q+m \cdot u_0)}{m-Z_{\dot{w}}} \right] & \frac{-M_{\dot{w}} mg \sin \theta}{I_y (m-Z_{\dot{w}})} \\ 0 & 0 & 1 & 0 \end{bmatrix} \begin{bmatrix} \Delta u \\ w \\ q \\ \theta \end{bmatrix} + \begin{bmatrix} \frac{\Delta X_c}{m} \\ \frac{\Delta Z_c}{m-Z_{\dot{w}}} \\ \frac{\Delta M_c}{I_y} + \frac{M_{\dot{w}}}{I_y} \frac{\Delta Z_c}{m-Z_{\dot{w}}} \\ 0 \end{bmatrix} \quad (1)$$

$$\begin{bmatrix} \dot{v} \\ \dot{p} \\ \dot{r} \\ \dot{\phi} \end{bmatrix} = \begin{bmatrix} \frac{Y_v}{m} & \frac{Y_p}{m} & \frac{Y_r}{m} - u_0 & g \cdot \cos \theta \\ \frac{L_v}{I'_x} + I'_{zx} N_v & \frac{L_p}{I'_x} + I'_{zx} N_p & \frac{L_r}{I'_x} + I'_{zx} N_r & 0 \\ I'_{zx} L_v + \frac{N_v}{I'_z} & I'_{zx} L_p + \frac{N_p}{I'_z} & I'_{zx} L_r + \frac{N_r}{I'_z} & 0 \\ 0 & 0 & \tan \theta & 0 \end{bmatrix} \begin{bmatrix} v \\ p \\ r \\ \phi \end{bmatrix} + \begin{bmatrix} \frac{\Delta Y_c}{m} \\ \frac{\Delta L_c}{I'_x} + I'_{zx} \Delta N_c \\ I'_{zx} \Delta L_c + \frac{\Delta N_c}{I'_z} \\ 0 \end{bmatrix} \quad (2)$$

$$I'_x = \frac{(I_x I_z - I_{zx}^2)}{I_z}; \quad I'_z = \frac{(I_x I_z - I_{zx}^2)}{I_x}; \quad I'_{zx} = \frac{I_{zx}}{(I_x I_z - I_{zx}^2)}.$$

It's also necessary, for the scaling, that the angle of attack, the lateral side-slip angle, the position of the control surface to be the same, which leads to a convenient choice for the reference movement: horizontal, rectilinear unaccelerated flight. In this case, one can express the variation of stability derivatives with the Reynolds number or, for same speed, the variation of the stability derivatives with the model scale.

## 2. RELATIVE DENSITY FACTOR SCALING

As shown in the reference [4], the relative density factor,  $\frac{m}{\rho l^3}$  is a basic similitude parameter in the aerodynamic forces. This factor is important in studying the phenomenon of flutter, but also in studying the characteristics of stability and control. The relative moment of inertia,  $\frac{I}{\rho l^5}$  has the same significance for the equations of the moment as the relative density factor has for the equations of the forces. Starting from:

$$I_y \dot{q} = \frac{1}{2} V^2 S c C_m \quad (3)$$

in dimensional format it follows:

$$C_m = 2 \left( \frac{I_y}{\rho S c} \right) \left( \frac{\dot{q}}{V^2} \right) = 2 \left( \frac{I_y}{\rho S c^3} \right) \left( \frac{\dot{q} c^2}{V^2} \right) = f \left( \frac{I_y}{\rho l^5}, \frac{\dot{\Omega} l^2}{V^2} \right), \quad (4)$$

$$C_m = f \left[ \frac{m}{\rho l^3}, \left( \frac{k}{l} \right)^2, \frac{\dot{\Omega} l^2}{V^2} \right]. \quad (5)$$

For the scaled model to have the same moment coefficient as the full-scale UAV, the relative moment of inertia,  $\frac{I}{\rho l^5}$ , and the reduced angular acceleration,  $\frac{\dot{\Omega} l^2}{V^2}$ , must be identical. For a rigid airplane, the moment of inertia can be adjusted by redistributing the masses inside the airplane in order to have the same  $K/L$  ratio, if the relative density factor is already met. In this case, this criterion provides us with a relation between airplane scale (parameter  $f_s$ ) and the airplane mass (parameter  $p_1$ ).

$$\frac{m_1}{\rho l_1^3} = \frac{m_2}{\rho l_2^3}, \text{ where } m_2 = m_1 \cdot p_1, l_2 = l_1 \cdot f_s. \quad (6)$$

Thus, we have a relation between  $f_s$  and  $p_1$ :

$$\frac{m_1}{\rho l_1^3} = \frac{m_2}{\rho l_2^3} \Leftrightarrow \frac{m_1}{l_1^3} = \frac{m_1 \cdot p_1}{(l_1 \cdot f_s)^3} \Leftrightarrow p_1 = f_s^3. \quad (7)$$

From this relation it results a method for scaling the UAVs by fulfilling the relative density factor criteria. This relation is added to the equations system and it is to be seen how mass distribution varies. Using MATLAB formulation can solve the system of equations for  $p_2$ . For example, for a scale factor of 2, to comply with the relative density criteria, we will obtain a value for  $p_2$  of 8 (see (5)–(6)).

### 3. SHORT-PERIOD MODE HYPOTHESIS SCALING

If we consider the short-period mode equations, as illustrated in the reference [13], the following formulas are obtained for  $\zeta_{sp}$  – the damping factor and  $\omega_{nsp}$  – undamped natural frequency. If our purpose is to have the same dynamic behavior both for the model plane and for the full-scale UAV, then we should have the same values for  $\zeta_{sp}$  and  $\omega_{nsp}$ . Having the results for the full-scale UAV, then we can determine the model parameters  $f_s$ ,  $p_1$  and  $p_2$  for the same  $\zeta_{sp}$  and  $\omega_{nsp}$  values in short-period mode approximation.

$$\begin{bmatrix} \dot{w} \\ \dot{q} \end{bmatrix} = \begin{bmatrix} \frac{Z_w}{m_{av}} & u_0 \\ \frac{1}{I_y} \left( M_w + \frac{M_{\dot{w}} Z_w}{m_{av}} \right) & \frac{1}{I_y} (M_q + M_{\dot{w}} u_0) \end{bmatrix} \cdot \begin{bmatrix} w \\ q \end{bmatrix}, \quad (8)$$

$$\lambda^2 - \lambda \left( \frac{Z_\alpha}{m_{av} u_0} + \frac{M_q}{I_y} + \frac{M_{\dot{\alpha}}}{I_y} \right) + \left( \frac{Z_\alpha}{m_{av} u_0} \frac{M_q}{I_y} - \frac{M_\alpha}{I_y} \right) = 0, \quad (9)$$

$$\zeta_1 = \frac{\frac{Z_\alpha}{m_{av} u_0} + \frac{M_q}{I_y} + \frac{M_{\dot{\alpha}}}{I_y}}{2 \cdot \omega_{nsp}} = -\frac{\lambda_1 + \lambda_2}{2 \cdot \omega_{nsp}} = \zeta_2 = \zeta_{sp}, \quad (10)$$

$$\omega_{n1} = \sqrt{\frac{Z_\alpha}{m_{av} u_0} \frac{M_q}{I_y} - \frac{M_\alpha}{I_y}} = \sqrt{\lambda_1 \cdot \lambda_2} = \omega_{n2} = \omega_{nsp}. \quad (11)$$

Here  $\zeta_2$  and  $\omega_{n2}$  are the values for the full-scale UAV (input values), and  $\zeta_1$  and  $\omega_{n1}$  for the scaled model. Knowing that:

$$\begin{aligned}\frac{M_q}{I_y} &= \frac{\frac{1}{4}\rho u_0 c m a^2 S C_{mq}}{I_y}, \\ \frac{Z_\alpha}{m_{av} u_0} &= \frac{u_0 \cdot Z_w}{m_{av} u_0} = \frac{\frac{1}{2}\rho u_0 S C_{Z\alpha}}{m_{av}}, \\ \frac{M_\alpha}{I_y} &= u_0 \cdot \frac{M_w}{I_y} = \frac{u_0 \frac{1}{2}\rho u_0 c m a S C_{m\alpha}}{I_y}, \\ \frac{M_{\dot{\alpha}}}{I_y} &= u_0 M_{\dot{w}} = \frac{u_0 \frac{1}{4}\rho c m a^2 S C_{m\dot{\alpha}}}{I_y}.\end{aligned}\quad (12)$$

with the following relations, we obtain  $\zeta_{sp}$  and  $\omega_{nsp}$  as a function of  $f_s$ ,  $p_1$  and  $p_2$ :

$$\begin{aligned}\omega_{nsp} &= \sqrt{\frac{Z_\alpha}{m_{av} u_0} \frac{M_q}{I_y} - \frac{M_\alpha}{I_y}} = \sqrt{\frac{\frac{1}{2}\rho u_0 S C_{Z\alpha}}{m_{av}} \frac{\frac{1}{4}\rho u_0 c m a^2 S C_{mq}}{I_y} - \frac{u_0 \frac{1}{2}\rho u_0 c m a S C_{m\alpha}}{I_y}} = \\ &= \frac{\rho u_0 S c m a}{2} \sqrt{\frac{1}{I_y} \left( \frac{C_{Z\alpha} C_{mq}}{2m_{av}} - \frac{2C_{m\alpha}}{\rho S c m a} \right)},\end{aligned}\quad (13)$$

$$\zeta_{sp} = \frac{\frac{Z_\alpha}{m_{av} u_0} + \frac{M_q}{I_y} + \frac{M_{\dot{\alpha}}}{I_y}}{2 \cdot \omega_{nsp}} = \frac{\frac{C_{Z\alpha}}{c m a m_{av}} + \frac{c m a (C_{m\dot{\alpha}} + C_{mq})}{2 I_y}}{\sqrt{\frac{1}{I_y} \left( \frac{C_{Z\alpha} C_{mq}}{2m_{av}} - \frac{2C_{m\alpha}}{\rho S c m a} \right)}}.\quad (14)$$

A quick conclusion is that if  $p_2$  is fixed and the relations between  $f_s$  and  $p_1$  complies with relative density similitude criteria ( $p_1 = f_s^3$ ), then the damping factor ( $\zeta_{sp}$ ) does not depend on the plane scale, which represents a first step in the behavior evaluation of the dynamic similitude between the full scale UAV and the scaled model. This fact is represented in the formula (15),

$$\zeta_{sp2} = \frac{\frac{C_{Z\alpha}}{c m a_1 \cdot f_s \cdot m_{av1} \cdot p_1} + \frac{c m a_1 \cdot f_s \cdot (C_{m\dot{\alpha}} + C_{mq})}{2 \cdot I_{y1} \cdot f_s^2 \cdot p_1 \cdot p_2}}{\sqrt{\frac{1}{I_{y1} \cdot f_s^2 \cdot p_1 \cdot p_2} \left( \frac{C_{Z\alpha} C_{mq}}{m_{av1} \cdot p_1} - \frac{2C_{m\alpha}}{\rho \cdot S_1 \cdot f_s^2 \cdot c m a_1 \cdot f_s} \right)}} = \frac{1}{f_s^4} \left( \frac{C_{Z\alpha}}{c m a_1 \cdot m_{av1}} + \frac{c m a_1 \cdot (C_{m\dot{\alpha}} + C_{mq})}{2 \cdot I_{y1}} \right) = \zeta_{sp1} \quad (15)$$

#### 4. ESTIMATION OF $p_1$ AND $p_2$ PARAMETERS

In this chapter we will estimate  $p_1$  and  $p_2$  of the model for a fixed scale  $f_s$ . Using step response dynamic of the full-scale UAV, this method estimates the model parameters  $f_s$ ,  $p_1$  and  $p_2$  using two methods.

First method is using the short-period mode approximation and the input equalities involves that  $\zeta_{sp}$  (damping factor) and  $\omega_{nsp}$  (undamped natural frequency) of the model have the same value as the  $\zeta_{sp}$  and

$\omega_{nsp}$  of the full-scale UAV. First method, although is having a theoretical basis, is an approximate method because it uses only short period mode from longitudinal channel (only  $2 \times 2$  matrix – [13]).

Second method uses full dynamic model. This implies use of both longitudinal and lateral-directional channel, each of which implies a  $4 \times 4$  matrix. So, in total we have four roots for each channel. For a stable plane, in longitudinal case we have four complex roots  $\lambda = n \pm i \cdot w$ , and in lateral-directional case we have two real roots (roll and spiral mode) and two complex roots (Dutch roll). In order to have the same dynamic behavior, eigenvalues ( $\lambda$ ) need to be the same, i.e. to have equality between the real parts and the imaginary parts. Considering the above it results 8 equalities that needs to be fulfilled (longitudinal and lateral channel). In the first method there are only two equalities.

In both situations, for solving the nonlinear system a MATLAB program is used. Dynamic model was implemented, and a first observation would be that if we keep the same scale factor for gravity center position, then certain aerodynamic coefficients remain quasi-constants. This aspect is illustrated in Fig. 1 and we can say that the coefficients  $C_L, C_{L0}, C_L^\alpha, C_L^{\delta e}, C_m, C_m^\alpha, C_m^{\delta e}$  do not change with the scale variation. It also helps that the studied aircraft is a flying wing and the difference in drag resulted from Reynolds variation does not significantly influence the moment coefficient. In order to illustrate Reynolds influence in airplane scale the polars  $C_L(C_D)$  were estimated in XFLR for various airplane scales. If the scaling method used obeys relative density factor, then an increase in airplane scale means an increase in Reynolds number, thus resulting in a lower drag coefficient. Since a dynamic model evaluation was considered depending on the step response, thus resulting in equality of the eigenvalues, dynamic model forces and moments needed to be estimated depending on the Reynolds number.

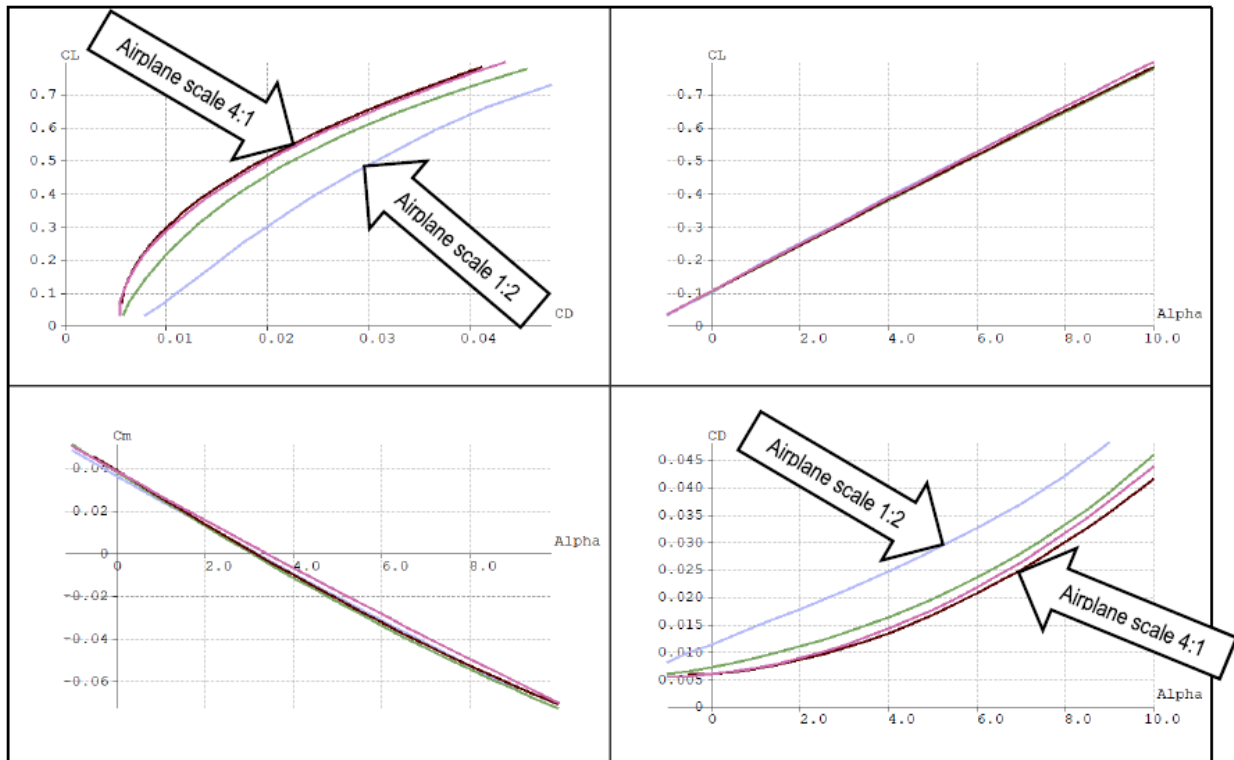


Fig. 1 – Model plane aerodynamic characteristics at various scales. XFLR polars.

#### 4.1. Estimation of $p_1$ and $p_2$ parameters – short-period mode approximation

In Table 1 the results from MATLAB program are summarized. Since the reference airplane is the model plane,  $f_s = 1$  is considered for the model plane. Equality conditions  $\omega_{nsp}$  and  $\zeta_{sp}$  are also calculated depending on the plane model parameters and the scale of the full-scale UAV. To better illustrate this, let's

look to an example: if you have a  $2\times$  scale ratio between the real UAV and the model plane, then, in order to have the same values for  $\omega_{nsp}$  and  $\zeta_{sp}$ , the model mass is multiplied by  $p_1 = 2.75$  and the inertia moment  $I_y$  is multiplied by 2.25. The values can be used to obtain a model plane, this plane can be used to conduct flight tests, in order to validate the theoretical results.

Table 1  
Scaling parameter values

Plane model ( $f_s = 1$ )		Equality conditions		Real Airplane (scaled)	
$p_1$	$p_2$	$\omega_{nsp}$	$\zeta_{sp}$	$f_s$ full-scale UAV	$p_1$ full-scale UAV ( $p_2 = 1$ )
1	1	7.08328	0.700643	1	1
1.8831	1.6398	5.7835	0.700643	1.5	3.375
2.7451	2.2524	5.0086	0.700643	2	8
3.6035	2.8585	4.4799	0.700643	2.5	15.625
4.4607	3.4618	4.0895	0.700643	3	27
5.3173	4.0638	3.7862	0.700643	3.5	42.875
6.1737	4.6651	3.5416	0.700643	4	64

From Table 1, we can say that the real UAV, built by scaling the model plane used in flight tests, has the same damping factor  $\zeta_{sp}$  and the same natural undamped frequency  $\omega_{nsp}$ . An important observation is that the variation of the parameters  $p_1$  and  $p_2$  with  $f_s$  is quasi-linear, which means that the method can be extrapolated with very small errors.

#### 4.2. Estimation of $p_1$ and $p_2$ parameters – full dynamic model

In this chapter the same concept is considered but the equality conditions include all the eigenvalues, both on longitudinal and lateral-directional channel. Table 2 has the results from the MATLAB code. As expected, for perturbations corresponding to the short-period mode ( $u, q$ ), the results are similar with errors less than 1%. If we refer to the perturbation evolution related to the phugoid mode, then the differences are slightly larger and reach up to 17%. These differences are best illustrated in the example above on the numeric values of the eigenvalues  $\lambda$ , but also in Fig. 3 – Fig. 5.

As input data, we have the UAV geometry multiplied by the scale factor, at which we add the mass and the moment of inertia weighted by the parameters  $p_1$  and  $p_2$ . In addition to the Etkin dynamic model, that was implemented, we also have the equalities conditions that the MATLAB function “Lsqnonlin” is trying to satisfy. This means that we have not been able to achieve equality but only the best approximation of the terms of equality within the meaning of the smallest squares method thus resulting the output variables  $p_1$  and  $p_2$  for the model plane. What is interesting is that although the solution is an approximate one, for various values of  $f_s$  we obtain a linear variation for  $p_1$  and  $p_2$ .

Table 2  
Scaling coefficients, complete matrices

Model plane ( $f_s = 1$ )				Real Airplane (scaled)	
$p_1$	$p_2$	$\omega_{nsp}$	$\zeta_{sp}$	$f_s$ Real airplane	$p_1$ Real Airplane ( $p_2 = 1$ )
1	1	7.08328	0.700643	1	1
1.3409	1.4782	5.970743	0.789368	1.5	3.375
1.6633	1.9503	5.268417	0.840095	2	8
1.9986	2.4235	4.769694	0.869236	2.5	15.625
2.3344	2.8959	4.391543	0.888891	3	27
2.6702	3.3679	4.091659	0.903106	3.5	42.875
3.0064	3.8394	3.846285	0.913834	4	64

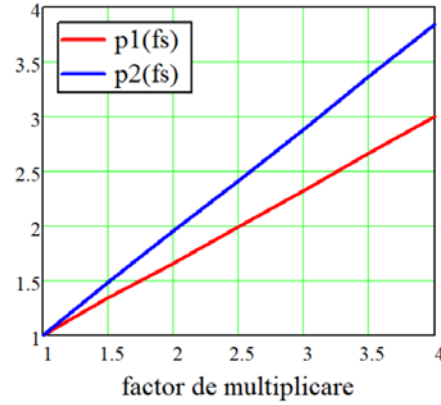


Fig. 2 – Variation of parameters  $p_1$  and  $p_2$  with scale factor – Complete matrices.

In order to further illustrate the methodology used we will take as an example the multiplication factor 1.5 ( $p_1 = f_s^3 = 3,375$ ,  $p_2 = 1$ ), resulting in a real plane with the following specifications:

Table 3  
Full-scale airplane specifications

Properties	Value	U.M.
Airplane mass	$10.517 \cdot p_1 = 35.5$	kg
Wing surface	$1.577 \cdot f_s^2 = 3.55$	m <sup>2</sup>
Wingspan	$4 \cdot f_s = 6$	m
Moment of inertia $I_y$	$1.35 \cdot f_s^2 \cdot p_1 \cdot p_2 = 10.25$	kg · m <sup>2</sup>

For this generated plane, the following eigenvalues resulted:

$$\lambda_L = \begin{Bmatrix} -3.283056 + 5.612509i \\ -3.283056 - 5.612509i \\ -0.020659 + 0.615824i \\ -0.020659 - 0.615824i \end{Bmatrix}, \quad \lambda_{LD} = \begin{Bmatrix} -0.068694 + 1.585213i \\ -0.068694 - 1.585213i \\ -0.141647 \\ -0.0000148 \end{Bmatrix}.$$

For this full-scale aircraft, we have the following specifications for the scaled model. The multiplier coefficients were presented in Table 4.

Table 4  
Model plane specifications

Properties	Value	U.M.
Airplane mass	$10.517 \cdot 1.3409 = 14.1$	kg
Wing surface	1.577	m <sup>2</sup>
Wingspan	4	m
Moment of inertia $I_y$	$1.35 \cdot 1.3409 \cdot 1.4782 = 2.676$	kg · m <sup>2</sup>

The resulting eigenvalues are:

$$\lambda_L = \begin{Bmatrix} -3.2596 + 5.6153i \\ -3.2596 - 5.6153i \\ -0.0249 + 0.6594i \\ -0.0249 - 0.6594i \end{Bmatrix}, \quad \lambda_{LD} = \begin{Bmatrix} -0.0584963 + 1.5984166i \\ -0.0584963 - 1.5984166i \\ -0.151769 \\ -0.00000929 \end{Bmatrix}$$

The major differences in the eigenvalues between the model and the actual plane are those related to phugoid mode, a percentage difference of not more than 17%. The best approximation is obtained for the short-period mode with differences of less than 1%, which is above the errors and approximations that have gathered along the way.

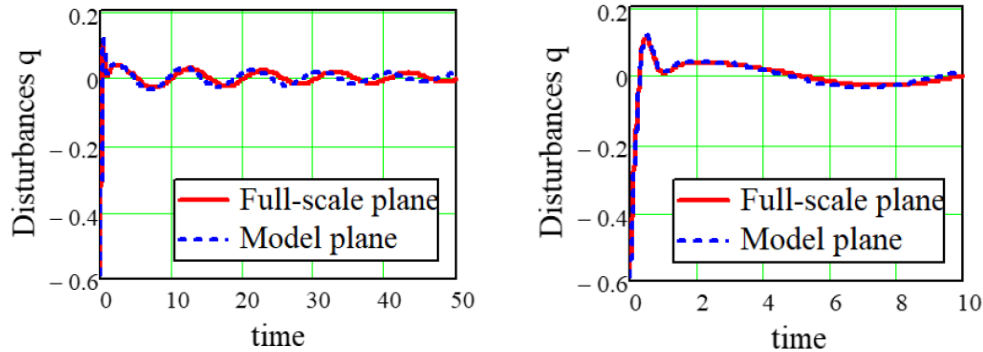


Fig. 3 – Step response comparison –  $q$  perturbations.

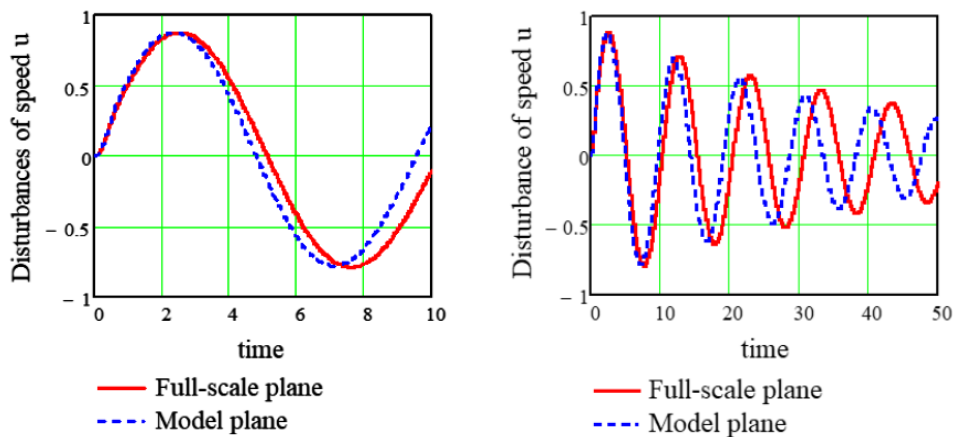


Fig. 4 – Step response comparison –  $u$  perturbations.

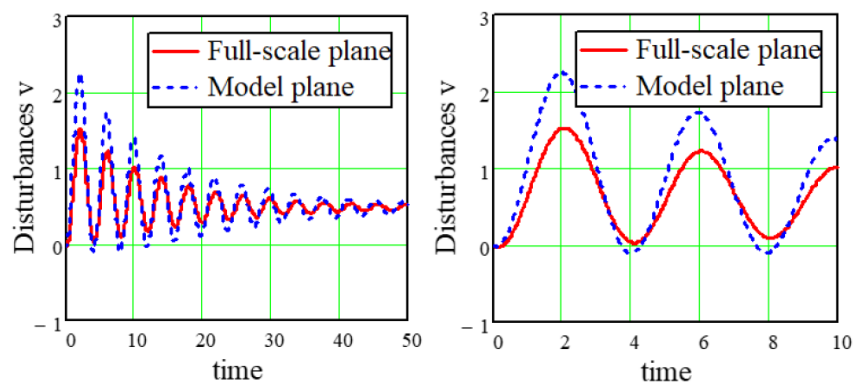


Fig. 5 – Step response comparison –  $v$  perturbations.

## 5. CONCLUSIONS

With additional inputs, the scaling method can be applied to any plane configuration, not only flying wing but also taking into consideration the error margin. The step response difference is insignificant regarding to the short period mode.



The method is more suitable for creating multiple versions of the same airplane at different scales. This greatly reduces the research and development costs. However, the method is less adequate for high scale ratios because the step response differences are also high.

Ultimately, the purpose is to perform fly tests using the same model plane with desired scale and mass parameters in order to validate the theoretical results. This paper supplies the model plane parameters to achieve this goal.

## REFERENCES

1. B. ETKIN, L.D. REID, *Dynamics of flight stability and control*, Third edition, John Wiley & Sons, 1996.
2. R.C. NELSON, *Flight stability and automatic control*, McGraw-Hill Book Company, 1989.
3. P. PARVU, *Mecanica zborului aeronavelor*, 2018; <https://aero.curs.pub.ro/2018/course/view.php?id=123>, accessed January 2020.
4. C.H. WOLOWICZ, J.S. BROWN JR, W.P. GILBERT, *Similitude requirements and scaling relationships as applied to model testing*, NASA technical paper 1435, Dryden Flight Research Center and Langley Research Center, 1979.
5. J. SANWALE, D.J. SINGH, *Aerodynamic parameters estimation using radial basis function neural partial differentiation method*, Defence Science Journal, **68**, 3, pp. 241–250, May 2018.
6. H. BENYAMEN, *Stability and control derivatives identification for an Unmanned Aerial Vehicle with low cost sensors using an Extended Kalman Filter algorithm*, M.Sc. Thesis, University of Kansas, 2019.
7. A. SRIVASTAVA, A. KUMAR, A.K. GHOSH, *Estimation of longitudinal aerodynamic derivatives using genetic algorithm optimized method*, American Journal of Engineering and Technology Management, **4**, 2, pp. 34–46, 2019.
8. A. HALANAY, A. IONIȚĂ, *Existence and stability of periodic motions in some roll-coupling dynamics of an aircraft*, Proceedings of the Romanian Academy, Series A: Mathematics, Physics, Technical Sciences, Information Science, **11**, 2, pp. 103–107, 2010.
9. S. GUDMUNDSSON, *General aviation aircraft design: Applied methods and procedures*, Elsevier, 2014.
10. M. LUNGU, R. LUNGU, *Reconfigurable controller for active fault-tolerant control systems with applicability to flight control*, Proceedings of the Romanian Academy, Series A: Mathematics, Physics, Technical Sciences, Information Science, **15**, 2, pp. 191–199, 2014.
11. R. LUNGU, M. LUNGU, C. ROTARU, *Non-linear adaptive system for the command of the helicopters pitch's angle*, Proceedings of the Romanian Academy, Series A: Mathematics, Physics, Technical Sciences, Information Science, **12**, 2, pp. 133–142, 2011.
12. M.V. COOK, *Flight dynamics principles*, Third edition, Elsevier Ltd., 1997.
13. D. RAYMER, *Aircraft design: A conceptual approach*, American Institute of Aeronautics and Astronautics, Inc., Washington, D.C., 1989.

Received January 26, 2020

